J Dent Mater Tech 2025; 14 (4): 187-196
DOI: 10.22038/JDMT.2025.90813.1881

J Dent Mater Tech

Original Article Open Access

Nano-hydroxyapatite modification of mineral trioxide aggregate (MTA): Physicochemical and biological evaluation of experimental endodontic cements

Chaitali Umesh Hambire[1]*, Umesh Vishnu Hambire [2]

Abstract

Objective: This study aimed to compare two Nano-hydroxyapatite (nHAp)-modified MTA systems (an additive formulation and a replacement formulation) against conventional MTA in terms of their physicochemical, cytocompatibility, and antimicrobial properties.

Methods: In this in-vitro study, three groups were evaluated: control MTA, a replacement nHAp-modified MTA group (MTA-nHAp-R, containing 35 wt% nHAp as a replacement), and an additive nHAp-modified MTA group (MTA-nHAp-A, containing 35 wt% nHAp as an additive). Standardized ISO-based protocols were employed to assess various cement properties, including compressive strength (24 hours and 7 days), setting time, radiopacity, pH (24 hours and 28 days), calcium ion release (24 hours, seven days and 28 days), surface morphology, cytotoxicity, and antibacterial activity (against Enterococcus faecalis and Staphylococcus epidermidis).

Results: At 7 days, the MTA-nHAp-A group exhibited significantly higher compressive strength compared to both the control and MTA-nHAp-R groups ($P<0.05$). The MTA-nHAp-R group had a significantly longer setting time and lower pH and calcium ion release compared to both the control and MTA-nHAp-A groups ($P<0.05$), which showed comparable values at most comparisons ($P>0.05$). Radiopacity, cytocompatibility and antibacterial activity of both nHAp-modified MTA formulations were comparable to conventional MTA ($P>0.05$). The MTA-nHAp-A group showed enhanced apatite deposition on SEM images.

Conclusions: Incorporation of nHAp into MTA either as additive incorporation (MTA-nHAp-A) or replacement incorporation (MTA-nHAp-R) significantly influenced its physicochemical properties. MTA-nHAp-A could serve as a promising alternative to MTA for endodontic applications due to its higher compressive strength at 7 days. However, replacing MTA powder with nHAp impairs MTA's mechanical performance.

Keywords: Antibacterial activity, Calcium release, Cytotoxicity, Mineral trioxide aggregate, Nano-hydroxyapatite, Root repair cement

Introduction

Mineral trioxide aggregate (MTA) was introduced in the 1990s as a hydraulic calcium silicate–based cement specifically developed for endodontic applications. MTA has been widely employed in clinical procedures such as root-end filling, perforation repair, apexification, and direct pulp capping. It demonstrates optimal ability to induce hard tissue deposition, promote periodontal regeneration, and maintain biocompatibility with pulpal and periapical tissues (1, 2). Despite these advantages, conventional MTA presents notable limitations, including prolonged setting times, difficult handling, tooth discoloration, solubility issues, and reduced compressive strength (3).

To address these limitations, research has focused on modifying MTA composition through the addition of bioactive components or partial substitution of silicate phases. Nano-hydroxyapatite (nHAp) has emerged as one of the most promising bioactive additives for calcium silicate cements (4, 5).

Hydroxyapatite [$Ca_{10}(PO_4)_6(OH)_2$] is the main mineral component of dental hard tissues. Nananoscale hydroxyapatite 00particles provide a high surface area, increased reactivity, and structural similarity to biological apatite (6, 7). nHAp provides a stable template for apatite nucleation and can directly interact with the calcium silicate hydration (C-S-H) products formed by

[1] Department of Pediatric Dentistry, Government Dental College and Hospital, Aurangabad, Maharashtra, India.
[2] Department of Mechanical Engineering, Government College of Engineering, Aurangabad, Maharashtra, India.

*Corresponding Author: Chaitali Umesh Hambire
Email: chaitalikmirajkar@gmail.com

Accepted: 12 November 2025. Submitted: 28 August 2025.

MTA, enhancing gel development (8, 9). The biocompatibility of nHAp has been confirmed in several in vitro and in vivo studies, which showed that nHAp actively promotes cell attachment and proliferation through its enhanced surface area and nanoscale material properties (4, 6).

Evidence suggests that hydroxyapatite can accelerate hydration kinetics, modify calcium hydroxide availability, and enhance microstructural densification, resulting in reduced pore volume and improved matrix refinement (10). Although nHAp has been studied as an additive to calcium silicate cements (4, 11), only a few investigations have compared different incorporation strategies, specifically, whether nHAp should be added as a supplement or introduced through partial replacement of MTA phases.

The present study aimed to formulate two nHAp-modified MTA systems using different incorporation methods (additive and replacement approaches) and to evaluate the physicochemical, cytocompatibility, and antimicrobial properties of these formulations. The null hypothesis was that incorporating nHAp into MTA, either as a replacement or as an additive, would not significantly affect setting time, compressive strength, radiopacity, pH, cytocompatibility, or antibacterial activity compared with conventional MTA.

Materials and methods

This experimental in vitro study was conducted at the Department of Pediatric Dentistry, Government Dental College and Hospital, Aurangabad, Maharashtra, India, between March 2023 and February 2024. As the study did not directly involve human or animal subjects, ethical approval was obtained for the use of human cell lines (Institutional Ethics Committee approval no. ECR/684/Inst/MH/2014/RR-21 dated June 30, 2021; IEC approval no. 001121/GDCHA/EAC-TRE/EC/2025; CTRI/2025/04/040552), in accordance with the Declaration of Helsinki (2013 revision) and institutional biosafety guidelines.

Grouping

This study evaluated three cement formulations: one control and two experimental nHAp-modified MTA systems. Each group is described below with its specific composition.

Conventional MTA (Control group): The control group consisted of a commercially available MTA (ProRoot MTA, Dentsply Tulsa Dental, USA). ProRoot MTA contains tricalcium silicate, dicalcium silicate, tricalcium aluminate, tetracalcium aluminoferrite, bismuth oxide as the radiopacifier, and calcium sulfate.

Replacement nHAp-modified MTA (MTA–nHAp–R): This group was prepared by replacing 35 wt% of the reactive MTA phases with nHAp (particle size <100 nm and >99% purity) (Sigma-Aldrich, MA, USA).

Additive nHAp-modified MTA (MTA–nHAp–A): This group was prepared by adding 35 wt% nHAp to the unmodified MTA base.

The compositions of the tested groups are summarized in Table 1. All materials were subjected to physicochemical, cytocompatibility, and antibacterial evaluations in accordance with ISO standards for dental cements.

Specimen preparation

A powder-to-liquid ratio of 0.3 g powder to 1 mL water was used for both experimental groups and the control MTA group, in accordance with the manufacturer's instructions. Powders were weighed using a digital microbalance (MP200A, A&D Company, Japan) and hand-mixed with distilled water on a glass slab. For physicochemical testing, the materials were placed into cylindrical Teflon molds with dimensions specified by ISO standards:

- 4 mm × 6 mm for compressive strength testing
- 10 mm × 2 mm for setting time
- 8 mm × 1.5 mm for radiopacity

All specimens were gently compacted using stainless steel spatulas to minimize air entrapment, covered with glass plates, and stored at 37°C with 95% relative humidity until testing.

Sample size calculation

Table 1. Composition of test materials used in this study

Group	nHAp Content	MTA Phase	Composition
Control MTA	0 wt%	100% (standard)	Commercial MTA (ProRoot, Dentsply Tulsa Dental), consisting of C_3S, C_2S, C_3A, tetracalcium aluminoferrite, and calcium sulfate
MTA-nHAp-R	35 wt%	65% (reduced)	35% of MTA replaced by nHAp (nano-hydroxyapatite)
MTA-nHAp-A	35 wt%	100% (preserved)	35% nHAp added alongside MTA without reducing the MTA content

The sample size for the compressive strength test was calculated with G*Power v3.1 (Heinrich Heine University, Düsseldorf, Germany) based on the data obtained from a pilot study. Considering $\alpha = 0.05$ and a power of 80%, the sample size was determined as n = 6 specimens per group for each time point (24 hours and 7 days).

For other outcomes, sample size calculations were selected based on the minimum sample required according to established conventions in dental materials research and ISO protocols, as follows:

- Setting time (n = 3)
- Radiopacity (n = 5)
- pH measurement (n=5)
- Calcium ion release (n = 5)
- Scanning electron microscopy (SEM) (n = 3)
- Cytotoxicity (n = 3). This test was assessed through three independent experiments, each conducted in triplicate wells.
- Antibacterial assays (n = 3)

Compressive strength

Compressive strength was measured at 24 hours and 7 days using a universal testing machine (Instron 3366; Instron Corp., Canton, MA, USA) at a crosshead speed of 1 mm/min. Cylindrical specimens (4 × 6 mm) were mounted on a UTM, and results were reported in megapascals (MPa).

Setting time

Setting time was measured following ISO 6876:2012 using the indentation method with a Gilmore needle apparatus. Two needles were used: an initial needle weighing 113.4 g with a 2.12 mm tip diameter, and a final needle weighing 453.6 g with a 1.06 mm tip diameter. The initial setting time was defined as the time from mixing until the initial needle no longer left a visible indentation on the cement surface. The final setting time was recorded when the final needle failed to make an indentation. Each measurement was repeated three times per group (n = 3), and the mean setting time was calculated in minutes.

Radiopacity

Specimen radiopacity was measured according to ISO 6876:2012. Five specimens (8 mm diameter × 1.5 mm thickness) were placed on a digital radiographic sensor (Kodak RVG 6100, Carestream Health, Rochester, NY, USA) and exposed alongside an aluminum reference step wedge. The step wedge consisted of 10 aluminum steps with thicknesses ranging from 1 to 10 millimeters in 1 millimeter increments, all with 99.5% purity. This stepped design creates a calibration scale that allows conversion of specimen radiographic density values to equivalent aluminum thickness measurements. Radiographs were taken using an X-ray unit (Focus, Instrumentarium, Tuusula, Finland) set at 70 kVp, 7 mA, with an exposure time of 0.32 seconds and a target-to-film distance of 30 cm.

Digital images were analyzed using Image J software (NIH, Bethesda, MD, USA). The mean gray value (pixel intensity) from three regions of interest per specimen was compared against the calibration curve to determine the equivalent aluminum thickness. Radiopacity values were expressed in millimeters of aluminum (mm Al).

pH

pH was measured by immersing specimens in 5 mL of deionized water. Readings were taken at 24 hours and 28 days using a calibrated digital pH meter (Orion Star A211, Thermo Scientific, USA).

Calcium ion release

Calcium concentration was determined using inductively coupled plasma optical emission spectroscopy (ICP-OES; PerkinElmer Optima 8000, Waltham, MA, USA). Calibration standards were prepared by serial dilution of a certified 1000 mg/L calcium standard solution (Sigma-Aldrich, St. Louis, MO, USA) with 2% nitric acid, creating matrix-matched calibration standards at concentrations of 0.1, 1, 5, 10, 25, and 50 mg/L. Calcium was quantified by measuring the emission at 393.37 nm using axial viewing geometry, and the results were compared to the matrix-matched calibration curve (0.1–50 mg/L). Calcium concentrations were reported in mg/L and expressed as cumulative release relative to baseline.

Surface characterization

Surface microstructure was examined using scanning electron microscopy (SEM; Hitachi TM4000Plus II, Japan) after a 7-day immersion in simulated body fluid (SBF). Specimens were sputter-coated with gold and observed at an accelerating voltage of 15 kV and 1000 X magnification.

Cytotoxicity

In vitro cytotoxicity was evaluated according to ISO 10993-5:2009 using human periodontal ligament fibroblasts (hPDLFs). Cells at passages 3–5 were selected because early-passage cells maintain phenotypic characteristics and demonstrate appropriate sensitivity for biocompatibility testing. Cells were cultured in Dulbecco's Modified Eagle Medium (DMEM; Gibco, Thermo Fisher Scientific, Inc., MA, USA) supplemented with 10% fetal bovine serum (FBS; Gibco) and antibiotics (100 U/mL penicillin and 100 µg/mL streptomycin) at 37°C with 5% CO_2.

Material extracts were prepared by incubating sterilized disk specimens (10 mm diameter × 2 mm thickness) in serum-free DMEM at 37°C for 24 hours, using a surface area-to-volume ratio of 0.2 cm^2/mL. Serial dilutions of the extracts (100%, 50%, 25%, and 12.5%) were then prepared. hPDLFs were seeded at 1 × 10^4 cells per well in 96-well plates, allowed to attach for 24 hours, and subsequently exposed to the extracts for another 24 hours. Cell viability was assessed using the MTT assay and expressed as a percentage relative to untreated control cells. A viability of ≥70% was considered non-cytotoxic, in accordance with ISO 10993-5:2009.

Antibacterial activity

Antibacterial activity was evaluated against Enterococcus faecalis (ATCC 19434) and Staphylococcus epidermidis (ATCC 35984) using a biofilm model. Biofilms were cultured on sterile cellulose nitrate membrane filters (0.22 µm pore size) for 48 hours at 37°C in a humidified incubator. Sterilized cement specimens (n = 3 per group) were then placed in direct contact with the biofilms for 24 hours at 37°C to assess the interaction with the established biofilm.

After the exposure period, biofilm disruption was performed as follows: the membrane filters supporting the biofilms were transferred into sterile tubes containing 1 mL of sterile phosphate-buffered saline (PBS, pH 7.4). Biofilm samples were then sonicated for 5 minutes at 50 W in an ultrasonic bath (40 kHz) to detach the bacteria from the membrane surface. Following sonication, the samples were vortexed vigorously for 15 seconds to ensure complete resuspension of the bacterial cells and to disperse any remaining cell aggregates.

Serial 10-fold dilutions (from 10^{-1} to 10^{-8}) of the sonicated samples were prepared in sterile PBS. From each dilution, 100 µL were plated in duplicate onto brain heart infusion (BHI) agar plates. The plates were incubated at 37°C for 24 hours under aerobic conditions. Colony-forming units (CFUs) were counted on plates containing 30–300 colonies (the acceptable range for reliable colony counting).

Statistical analysis

The data were analyzed using IBM SPSS Statistics version 25.0 (IBM Corp., Armonk, NY, USA). Normality was confirmed with the Shapiro-Wilk test ($P > 0.05$). Group comparisons were performed using one-way ANOVA followed by Tukey's post hoc test. The significance level was set at $P < 0.05$.

Results

Compressive strength

Table 2 presents the mean and standard deviation (SD) of the compressive strength (MPa) at 24 hours and 7 days in the study groups. At 24 hours, the lowest compressive strength was observed in the MTA-nHAp-R group (28.9 ± 2.3 MPa), while the MTA-nHAp-A group showed the highest strength at this time point (35.8 ± 2.2 MPa). After 7 days, compressive strength increased in all groups. The MTA-nHAp-A group maintained the highest strength (68.4 ± 2.6 MPa), exceeding that of the control MTA group (55.3 ± 2.8 MPa) and the MTA-nHAp-R (52.7 ± 3.1 MPa) group also showed the lowest compressive strength.

One-way ANOVA revealed significant differences in compressive strength between groups at both 24 hours

Table 2. Mean ± standard deviation (SD) of the compressive strength (MPa) at 24 hours and 7 days in the study groups

Groups	24 hours	7 days
	Mean ± SD*	Mean ± SD*
Control MTA	32.6 ± 2.1[a,b]	55.3 ± 2.8[a]
MTA- nHAp-R	28.9 ± 2.3[a]	52.7 ± 3.1[a]
MTA-nHAp-A	35.8 ± 2.2[b]	68.4 ± 2.6[b]
P-value	<0.001	<0.001

*Different superscripted letters denote statistically significant differences between groups at P<0.05.
MTA-nHAp-R contains 35 wt% nHAp as a replacement.
MTA-nHAp-A contains 35 wt% nHAp as an additive.

Table 3. Mean ± standard deviation (SD) of the setting time (minutes) and radiopacity (mm of aluminum) in the study groups

Groups	Setting time	Radiopacity (mm Al)
	Mean ± SD	Mean ± SD
Control MTA	118 ± 3[a]	6.1 ± 0.2
MTA- nHAp-R	135 ± 4[b]	5.7 ± 0.3
MTA-nHAp-A	121 ± 3[a]	6.0 ± 0.3
P-value	0.002	0.09

*Different superscripted letters denote statistically significant differences between groups at P<0.05.
MTA-nHAp-R contains 35 wt% nHAp as a replacement.
MTA-nHAp-A contains 35 wt% nHAp as an additive.

and 7 days (P<0.001). Tukey's HSD post-hoc analysis showed that at 24 hours, the MTA-nHAp-A group had significantly higher compressive strength than the MTA-nHAp-R group (P < 0.05; Table 2). At 7 days, the MTA-nHAp-A group exhibited significantly higher compressive strength compared to both the control and MTA-nHAp-R groups (P < 0.05; Table 2).

Setting Time

Table 3 presents the mean and standard deviation (SD) of the setting time (min) in the study groups. All groups exhibited clinically acceptable setting times within the typical range for MTA-based cements. The control MTA had a mean setting time of 118 ± 3 minutes, while the MTA-nHAp-R group showed the longest setting time at 135 ± 4 minutes.

ANOVA revealed a significant difference in setting time among the groups (P=0.001). Tukey's HSD test indicated that the MTA-nHAp-R group had a significantly longer setting time compared to both the control and MTA-nHAp-A groups (P<0.05), whereas the setting times of the control and MTA-nHAp-A groups were comparable (P>0.05; Table 3).

Radiopacity

Table 3 presents the mean and standard deviation (SD) of the radiopacity (mm Al) in the study groups. All groups showed radiopacity values exceeding the ISO 6876 minimum requirement of 3 mm Al. The control MTA and MTA-nHAp-A exhibited similar radiopacity (6.1 ± 0.2 mm and 6.0 ± 0.3 mm Al, respectively), whereas MTA-nHAp-R had a slightly lower value (5.7 ± 0.3 mm Al). One-way ANOVA revealed no significant difference in radioopacity between the groups (P = 0.09; Table 3).

pH

Table 4 presents the mean and standard deviation (SD) of the pH at 24 hours and 28 days in the study groups. At all times, all groups maintained alkaline pH values throughout the testing period. At 24 hours, control MTA showed the highest pH (11.9 ± 0.1), followed by MTA-nHAp-A (11.7 ± 0.1), while MTA-nHAp-R exhibited a slightly lower value (11.4 ± 0.1). One-way ANOVA indicated a significant difference in pH between groups at 24 hours (P<0.001), with all groups differing significantly from each other (P<0.05; Table 4).

At 28 days, the highest pH was observed in the control group (11.8 ± 0.1), followed by the MTA-nHAp-A group (11.7 ± 0.1) and the MTA-nHAp-R group (11.5 ± 0.1). One-way ANOVA revealed a significant difference between the groups (P<0.01), with the MTA-nHAp-R

Table 4. Mean ± standard deviation (SD) of the pH at 24 hours and 28 days in the study groups

Groups	24 hours	28 days
	Mean ± SD*	Mean ± SD*
Control MTA	11.9 ± 0.1[c]	11.8 ± 0.1[b]
MTA- nHAp-R	11.4 ± 0.1[a]	11.5 ± 0.1[a]
MTA-nHAp-A	11.7 ± 0.1[b]	11.7 ± 0.1[b]
P-value	<0.001	<0.001

*Different superscripted letters denote statistically significant differences between groups at P<0.05.
MTA-nHAp-R contains 35 wt% nHAp as a replacement.
MTA-nHAp-A contains 35 wt% nHAp as an additive.

Table 5. Mean ± standard deviation (SD) of the calcium ion release ($mg \cdot L^{-1}$) at 24 hours, 7 days, and 28 days in the study groups

Groups	24 hours	7 days	28 days
	Mean ± SD	Mean ± SD	Mean ± SD
Control MTA	49.3 ± 1.4a	73.4 ± 1.3a	90.4 ± 1.3a
MTA- nHAp-R	32.8 ± 0.8b	52.0 ± 1.0b	65.0 ± 0.9b
MTA-nHAp-A	47.3 ± 0.9a	70.7 ± 0.9a	86.9 ± 1.2a
P-value*	<0.001	<0.001	<0.001

*Different superscripted letters denote statistically significant differences between groups at P<0.05.
MTA-nHAp-R contains 35 wt% nHAp as a replacement.
MTA-nHAp-A contains 35 wt% nHAp as an additive.

group showing a significantly lower pH than both the control group and the MTA-nHAp-A group (P<0.05, Table 4).

Calcium ion release

Table 5 presents the mean and standard deviation (SD) of the calcium ion release ($mg \cdot L^{-1}$) at 24 hours, 7 days, and 28 days in the study groups. At all times, control MTA released the highest calcium concentrations, while MTA-nHAp-R released the lowest. The MTA-nHAp-A group maintained calcium release levels close to those of the control group.

One-way ANOVA showed significant differences in calcium ion release between groups at all time points (P < 0.001). Pairwise comparisons revealed that the MTA-nHAp-R group had significantly lower calcium ion release than the other groups at all intervals (P < 0.05; Table 5).

Surface characterization

Scanning electron microscopy (SEM) examination revealed morphological differences between the groups. The control MTA exhibited needle-like crystalline structures on the specimen surface, suggesting the early stages of apatite formation (Figure 1A). The MTA-nHAp-R group presented irregular, agglomerated particle clusters, indicative of apatite-like mineral deposition but with less uniform organization (Figure 1B). The MTA-nHAp-A group displayed the most uniform and extensive globular particle deposition on the specimen surface, morphologically consistent with apatite formation (Figure 1C).

Cytotoxicity

The MTT assay revealed reduced cell viability at full-strength extracts (100%), with values ranging between 51–57%. At 50% extract concentration, viability improved across all groups to approximately 69–74%,

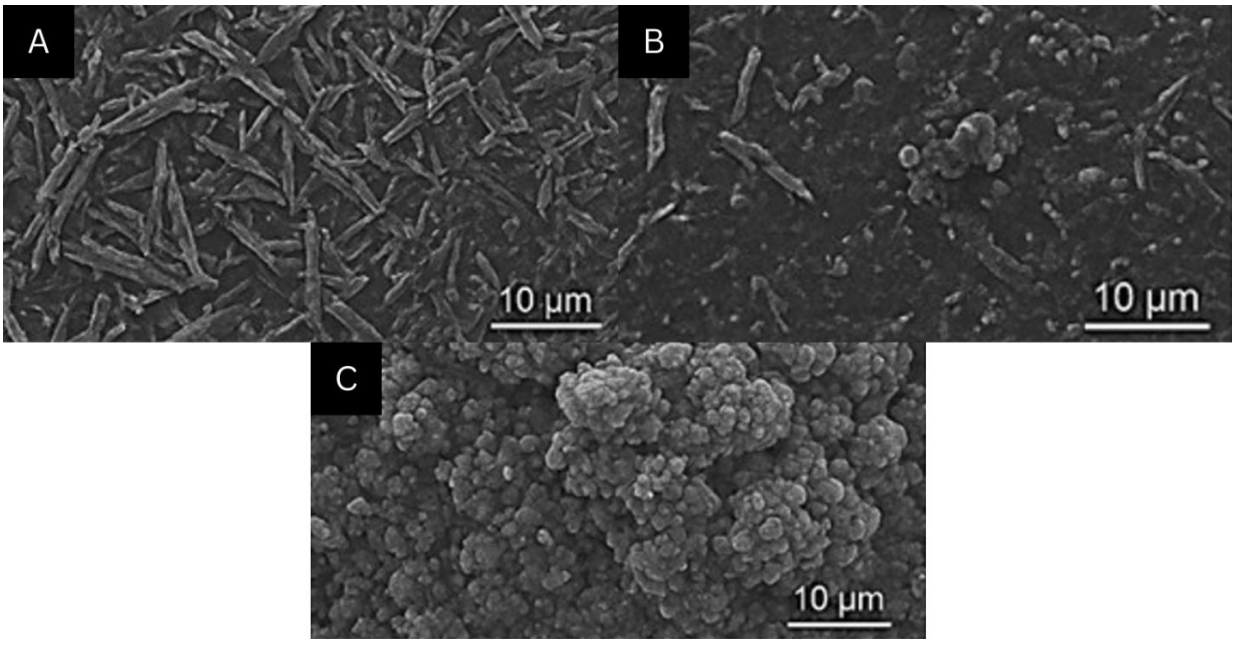

Figure 1. SEM micrographs after 7-day immersion of the study groups in simulated body fluid (SBF). A. Control MTA showing needle-like crystalline structures; B. MTA-nHAp-R showing irregular, agglomerated particle clusters; C. MTA-nHAp-A showing uniform and extensive globular particle deposits.

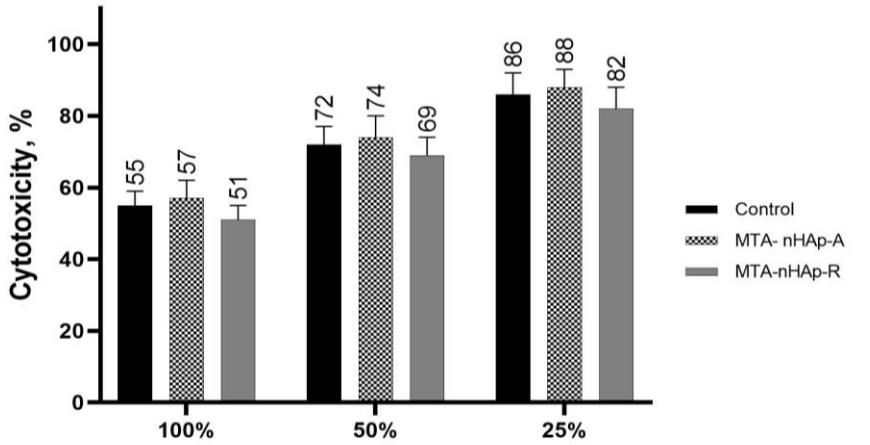

Figure 2. Cytotoxicity of material extracts on hPDLF cells at different dilutions (MTA-nHAp-A contains 35 wt% nHAp as an additive. MTA-nHAp-R, contains 35 wt% nHAp as a replacement.)

and at 25%, viability exceeded 82% for all materials tested. These results indicate that, except for the undiluted extracts, all cements met the ISO 10993-5 criteria for acceptable cytocompatibility. One-way ANOVA revealed no significant differences between groups at any concentration (P=0.30 at 100%; P=0.54 at 50%; and P=0.46 at 25%) (Figure 2).

Antibacterial activity

All groups exhibited antibacterial activity against *Enterococcus faecalis* and *Staphylococcus epidermidis*. A reduction greater than 2 $\log_{10}$ colony-forming units (CFU) was observed against *S. epidermidis*, while approximately a 1 $\log_{10}$ reduction was noted against *E. faecalis* across all groups. One-way ANOVA showed no significant differences between groups for either of the bacterial species (*E. faecalis*: P=0.25; *S. epidermidis*: P=0.72) (Figure 3).

Discussion

This study evaluated the physicochemical and biological performance of experimental MTA formulations modified with nano-hydroxyapatite. The findings partially rejected the null hypothesis, as nHAp incorporation significantly affected certain material properties, including compressive strength, setting time, pH, and calcium ion release, while radiopacity, cytotoxicity and antibacterial activity were not impacted. The concentration of nHAp in both the replacement and additive groups (35 wt%) was selected

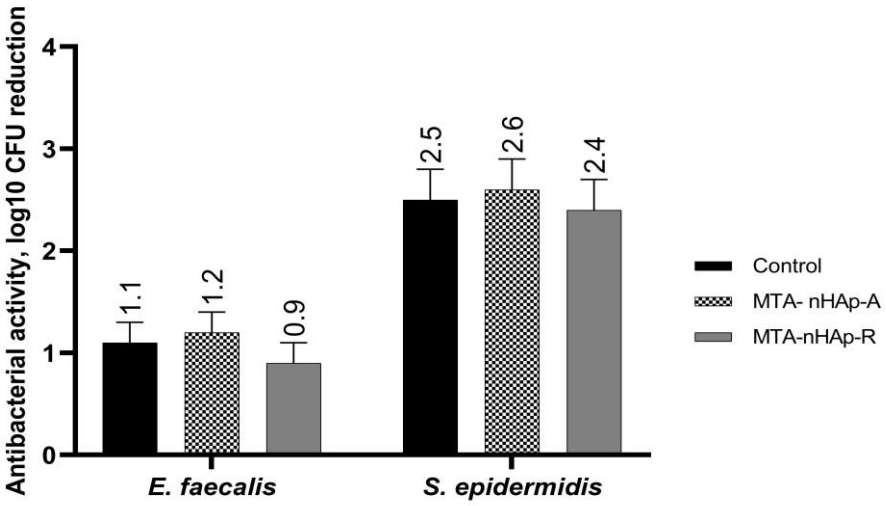

Figure 3. Antibacterial activity against *E. faecalis* and *S. epidermidis* (log10 CFU reduction) (MTA-nHAp-A contains 35 wt% nHAp as an additive. MTA-nHAp-R, contains 35 wt% nHAp as a replacement.)

to achieve a substantial modification of the MTA matrix while maintaining the core hydration mechanisms necessary for cement functionality (4, 11).

In the present study, the MTA-nHAp-A group had significantly higher compressive strength than the MTA-nHAp-R group at 24 hours. At 7 days, the MTA-nHAp-A group exhibited significantly higher compressive strength compared to both the control and MTA-nHAp-R groups. The higher compressive strength observed in the MTA-nHAp-A group compared to the control group and the MTA-nHAp-R group can be explained by the dual role of nHAp as both a micro-reinforcing filler and a nucleation site for calcium silicate hydrate (C–S–H) growth. When nHAp is added without replacing reactive MTA phases, it enhances particle packing and interfacial bonding, resulting in increased matrix density and strength. In contrast, in the replacement group (MTA-nHAp-R), the partial substitution of reactive tricalcium silicate with nHAp reduces the overall amount of hydration products formed. In this case, the reinforcing effect of nHAp is insufficient to compensate for the loss of reactive phases, leading to decreased mechanical strength. This explains why the additive approach improves strength, while replacement has a detrimental effect (11, 14).

The superior strength of MTA-nHAp-A is consistent with findings by Yong et al. (11), who developed an endodontic cement combining bovine bone-derived hydroxyapatite with Portland cement and assessed its mechanical properties. Although Yong et al. did not directly compare additive versus replacement methods, their observation aligns well with the current resuls, because they found that hydroxyapatite incorporation enhanced matrix densification and accelerated C–S–H formation through heterogeneous nucleation Similarly, Koutroulis et al. (15) reported that partial substitution of tricalcium silicate with hydroxyapatite reduced mechanical strength due to decreased hydration, while additive incorporation improved microstructural density and compressive strength.

The setting behavior of the experimental cements varied depending on the nHAp content and formulation approach. The MTA-nHAp-R group had a significantly longer setting time compared to both the control and MTA-nHAp-A groups, likely because replacing reactive tricalcium silicate with inert nHAp reduced the availability of calcium and silicate ions needed for early hydration and C–S–H gel formation. Conversely, the additive group (MTA-nHAp-A) showed a setting time comparable to the control MTA, indicating that introducing nHAp as an additional phase does not significantly disrupt the hydration process. These results highlight the importance of preserving sufficient reactive silicate content to maintain optimal setting kinetics in nHAp-modified MTA formulations (12, 13).

In this study, the MTA-nHAp-R group had significantly lower calcium ion release than the other groups at all intervals. The reduction in calcium ion release in the MTA-nHAp-R group compared to the other two groups is consistent with the lower tricalcium silicate content available for hydration and calcium hydroxide formation. The differential calcium ion release between formulations reflects differences in reactive silicate availability. In MTA-nHAp-A, the full complement of tricalcium and dicalcium silicate of MTA is preserved for normal hydration, producing calcium ions through silicate hydrolysis and subsequent calcium hydroxide formation (16).

The alkaline pH of MTA, mainly resulting from calcium hydroxide release, is crucial for its antibacterial properties and its ability to stimulate hard tissue formation (17). In this study, the MTA-nHAp-R group exhibited a slight reduction in both pH and calcium release, whereas the additive group (MTA-nHAp-A) maintained values comparable to the control. Guerreiro-Tanomaru et al. (4) reported that adding nano-hydroxyapatite particles at 10% and 20% concentrations did not significantly affect pH and the initial setting time of the Portland cement associated with zirconium oxide (ZrO_2). The present study is consistent with these findings, suggesting that incorporating nHAp as an additive rather than replacing reactive MTA components preserves the essential pH-generating mechanisms driven by calcium silicate hydration.

In the present study, no significant difference was found in radioopacity between the groups. Islam et al. (18) reported that ProRoot MTA maintained an alkaline pH throughout extended immersion periods, with radiopacity values ranging from 6.47 to 6.74 mm Al, similar to those observed in this study. Kaup et al. (19) reported a radiopacity of 6.40 ± 0.06 mm Al. In contrast, Guerreiro-Tanomaru et al. (4) reported that incorporation of nano-hydroxyapatite into calcium silicate cement formulations may enhance radiopacity by increasing matrix density and improving particle packing.

SEM analysis showed extensive apatite deposition, particularly in the additive group (MTA-nHAp-A), following 7-day immersion in simulated body fluid (SBF), highlighting the enhanced bioactivity due to nHAp incorporation. In contrast, the MTA-nHAp-R group

presented irregular and less uniform mineral deposition. The findings of this study are consistent with those reported by Gandolfi et al. (20), who evaluated the apatite-forming ability (bioactivity) of ProRoot MTA following immersion in SBF and identified similar apatite crystal deposition on the cement surface using SEM analysis. Yong et al. (11) also reported increased apatite deposition on hydroxyapatite-containing calcium silicate cements after immersion in simulated body fluid (SBF). However, their study did not differentiate between additive and replacement strategies.

Cytotoxicity assay confirmed that nHAp-modified cements maintain cytocompatibility comparable to control MTA. Although neat (100%) extracts reduced cell viability below the 70% threshold set by ISO 10993-5 for non-cytotoxicity, diluted extracts (50% and 25%) demonstrated cell viabilities exceeding this limit, indicating acceptable biocompatibility. The present findings agree with those of several studies that reported favorable cell compatibility of hydroxyapatite nanostructures (21, 22).

Antibacterial assays showed that the inherent alkalinity of MTA, a key factor in its antimicrobial efficacy, is preserved in nHAp-modified formulations (23, 24). As anticipated, *Enterococcus faecalis* exhibited greater resistance to the cements' antibacterial effects than *Staphylococcus epidermidis*, reflecting its well-documented capacity to survive in alkaline conditions (25).

This study, however, has some limitations, including its in vitro design, relatively short-term immersion protocols, and the lack of histological assessment. Further research is needed to evaluate long-term ion release and handling properties of this formulation to fully establish its suitability for clinical applications.

Conclusions

Under the conditions used in this study:

1. Incorporation of nHAp into MTA either as additive incorporation (MTA-nHAp-A) or replacement incorporation (MTA-nHAp-R) significantly influenced its physicochemical properties.
2. At 7 days, the MTA-nHAp-A group exhibited significantly higher compressive strength compared to both the control and MTA-nHAp-R groups.
3. The MTA-nHAp-R group had a significantly longer setting time and lower pH and calcium ion release compared to both the control and MTA-nHAp-A groups, which showed comparable values at most comparisons.
4. Radiopacity, cytocompatibility and antibacterial activity of both nHAp-modified MTA formulations were comparable to conventional MTA.
5. Overall, MTA-nHAp-A could serve as a promising alternative to MTA for endodontic applications due to its higher compressive strength at 7 days.

Acknowledgements

Not Applicable.

Conflict of interest

The authors declare no conflict of interest.

Author contributions

C.H.H. contributed to the research design, implementation, data collection, and writing of the manuscript. U.V.H. contributed to the research implementation, data analysis, data interpretation, and writing of the manuscript. All authors have read and approved the final manuscript.

Ethical considerations

As the study did not directly involve human or animal subjects, ethical approval was obtained for the use of human cell lines (Institutional Ethics Committee approval no. ECR/684/Inst/MH/2014/RR-21 dated June 30, 2021; IEC approval no. 001121/GDCHA/EAC-TRE/EC/2025; CTRI/2025/04/040552), in accordance with the Declaration of Helsinki (2013 revision) and institutional biosafety guidelines.

Funding

No funding was received for conducting this study.

References

1. Torabinejad M, Watson TF, Pitt Ford TR. Sealing ability of a mineral trioxide aggregate when used as a root end filling material. J Endod 1993;19(12):591-595.

2. Priyadharshini S, Ragavendran C, Sherwood A. The antibacterial properties and biocompatibility of carbonated hydroxyapatite as a pulp capping agent. J Dent Mater Tech 2025;14(1):35-42.

3. Parirokh M, Torabinejad M. Mineral trioxide aggregate: a comprehensive literature review--Part I:

chemical, physical, and antibacterial properties. J Endod 2010;36(1):16-27.
4. Guerreiro-Tanomaru JM, Vázquez-García FA, Bosso-Martelo R, Bernardi MI, Faria G, Tanomaru MF. Effect of addition of nano-hydroxyapatite on physico-chemical and antibiofilm properties of calcium silicate cements. J Appl Oral Sci 2016;24(3):204-210.
5. Saghiri MA, Orangi J, Asatourian A, Gutmann JL, Garcia-Godoy F, Lotfi M, et al. Calcium silicate-based cements and functional impacts of various constituents. Dent Mater J 2017;36(1):8-18.
6. Pushpalatha C, Gayathri VS, Sowmya SV, Augustine D, Alamoudi A, Zidane B, et al. Nanohydroxyapatite in dentistry: A comprehensive review. Saudi Dent J 2023;35(6):741-752.
7. Mobaleghi T, Vafadoost R, Sadeghi R, Mashhadi-Abbas F, Ahmadian-Moghadam H, Semyari H, et al. Histomorphometric and histologic evaluation of the effects of leukocyte platelet-rich fibrin (L-PRF) and nano-hydroxyapatite (nHA) on bone regeneration in rabbits. J Dent Mater Tech 2023;12(1):43-50.
8. Flores-Ledesma A, Tejeda-Cruz A, Bucio L, Wintergerst AM, Rodríguez-Chávez JA, Moreno-Vargas YA, et al. Hydration products and bioactivity of an experimental MTA-like cement modified with wollastonite and bioactive glass. Ceram Int 2020;46(10, Part B):15963-15971.
9. Dey A, Bomans PH, Müller FA, Will J, Frederik PM, de With G, et al. The role of prenucleation clusters in surface-induced calcium phosphate crystallization. Nat Mater 2010;9(12):1010-1014.
10. Lubojański A, Zakrzewski W, Samól K, Bieszczad-Czaja M, Świtała M, Wiglusz R, et al. Application of Nanohydroxyapatite in Medicine-A Narrative Review. Molecules 2024;29(23):5628.
11. Yong D, Choi JJE, Cathro P, Cooper PR, Dias G, Huang J, et al. Development and Analysis of a Hydroxyapatite Supplemented Calcium Silicate Cement for Endodontic Treatment. Materials (Basel) 2022;15(3):1176.
12. John E, Matschei T, Stephan D. Nucleation seeding with calcium silicate hydrate – A review. Cem Concr Res 2018;113:74-85.
13. Aretxabaleta XM, López-Zorrilla J, Etxebarria I, Manzano H. Multi-step nucleation pathway of C-S-H during cement hydration from atomistic simulations. Nat Commun 2023;14(1):7979.
14. Al-Saffar FY, Wong LS, Paul SC. An Elucidative Review of the Nanomaterial Effect on the Durability and Calcium-Silicate-Hydrate (C-S-H) Gel Development of Concrete. Gels 2023;9(8):613.
15. Koutroulis A, Menon N, Kapralos V, Ørstavik D, Pain M, Valen H, et al. Investigation of the effect of addition/replacement of bioactive glass to hydraulic calcium silicate cement. Dent Mater 2025;41(9):1067-1079.
16. Camilleri J. Characterization of hydration products of mineral trioxide aggregate. Int Endod J 2008;41(5):408-417.
17. Sharifi S, Dizaj SM, Shahi S, Mahdilouy M. Synthesis, characterization, and evaluation of nano-hydroxyapatite based experimental calcium silicate cement as a root repair material. J Oral Res (Impresa) 2022:1-13.
18. Islam I, Chng HK, Yap AU. Comparison of the physical and mechanical properties of MTA and portland cement. J Endod 2006;32(3):193-197.
19. Kaup M, Schäfer E, Dammaschke T. An in vitro study of different material properties of Biodentine compared to ProRoot MTA. Head Face Med 2015;11:16.
20. Gandolfi MG, Taddei P, Tinti A, Prati C. Apatite-forming ability (bioactivity) of ProRoot MTA. Int Endod J 2010;43(10):917-929.
21. Kovrlija I, Menshikh K, Abreu H, Cochis A, Rimondini L, Marsan O, et al. Challenging applicability of ISO 10993-5 for calcium phosphate biomaterials evaluation: Towards more accurate in vitro cytotoxicity assessment. Biomater Adv 2024;160:213866.
22. Yan X, Ebrahimi A, Mohammadi R, Tehrani MM, Chaboki P, Mustafa M, et al. Investigation of bioactivity, biocompatibility, and antibacterial properties of a hydroxyapatite-enhanced nanocomposite for dental applications. Sci Rep 2025;15(1):28557.
23. Bolhari B, Chitsaz N, Nazari S, Behroozibakhsh M, Sooratgar A, Hashemian A. Effect of Fluorohydroxyapatite on Biological and Physical Properties of MTA Angelus. Scientific World Journal 2023;2023:7532898.
24. Bolhari B, Sooratgar A, Pourhajibagher M, Chitsaz N, Hamraz I. Evaluation of the Antimicrobial Effect of Mineral Trioxide Aggregate Mixed with Fluorohydroxyapatite against E. faecalis In Vitro. Scientific World Journal 2021;2021:6318690.
25. Hiremath G, Pramanik S, Horatti P, Anil. Comparative evaluation of bioactivity of MTA plus and MTA plus chitosan conjugate in phosphate buffer saline an invitro study. Saudi Dent J 2024;36(8):1097-1104.